

1 **Extinction drives recent thermophilization but does not trigger**
2 **homogenization in forest understory**

3

4 Jeremy Borderieux^{1,*}, Jean-Claude Gégout¹, Josep M. Serra-Diaz^{1,2}

5 1. Université de Lorraine, AgroParisTech, INRAE, UMR Silva, 54000 Nancy, France

6 2. Eversource Energy Center and Department of Ecology and Evolutionary Biology,

7 University of Connecticut, Storrs, CT, United States of America

8 Orcid ID:

9 Jeremy Borderieux : 0000-0003-3993-1067

10 Jean-Claude Gégout : 0000-0002-5760-9920

11 Josep M. Serra-Diaz: 0000-0003-1988-1154

12

13 Corresponding author: Jeremy Borderieux: jeremy.borderieux@agroparistech.fr

14

15

16

17 **Abstract**

18

19 The ongoing climate change is triggering plant community thermophilization. Such selection
20 process towards warm-adapted species may also lead to biotic homogenization. The link
21 between those two processes and the community dynamic driving them (colonization and
22 extinction) remain unknown but are critical to understand community response under rapid
23 environmental change.

24 We used 12,764 pairs of plots to study plant community change in 16 years of rising
25 temperatures in 80 forest ecoregions of France. We computed thermophilization and $\Delta\beta$ -
26 diversity (homogenization) for each ecoregion, and partitioned these changes into extinction
27 and colonization dynamics for cold and warm-adapted species.

28 Forest understory communities thermophilized on average by $0.12\text{ }^{\circ}\text{C decade}^{-1}$ and up to 0.20
29 $^{\circ}\text{C decade}^{-1}$ in warm ecoregions. This rate was entirely driven by extinction dynamics.
30 Extinction of cold-adapted species was a driver of homogenization, but it was compensated
31 by the colonization of rare species and the extinction of common species. This results in a lack
32 of apparent trend of homogenization.

33 An extinction-driven thermophilization is concerning as it reflects the dieback of current
34 species rather than adaptation of understory to climate change. These results suggest that a
35 future loss of biodiversity and a delayed biotic homogenization should be considered.

36

37

38 **Keywords**

39

40 Community ecology, thermophilization, homogenization, β -diversity, climate change, forest,
41 understory.

42

43 1. Introduction

44 The unprecedented speed of the current climate warming is causing major biodiversity shifts and
45 the reshuffling of ecological communities (Lenoir & Svenning, 2015; Svenning & Sandel, 2013).
46 Such reshuffling could lead to a major risk for biodiversity worldwide (Sala et al., 2000) and
47 the services it provides (Reu et al., 2022; Wang et al., 2021). Two major patterns in community
48 composition have been reported as a result of global changes: thermophilization and biotic
49 homogenization. On the one hand, thermophilization of plant communities – the increase in
50 the average temperature affiliation of species in a community over time – is increasing as a
51 result of climate warming (De Frenne et al., 2013; Martin et al., 2019; Richard et al., 2021),
52 albeit at a slower pace than climate e.g. (Bertrand et al., 2011, 2016). In parallel, evidence
53 also suggests that biotic homogenization across plant communities is occurring (Cholewińska
54 et al., 2020; Olden & Rooney, 2006; Staude et al., 2022). This is evidenced by a decrease in
55 β -diversity, a measure that signal an increase of similarity among community of a region. To
56 date, whether these processes occur simultaneously, their linkages, and which community
57 dynamics underlie such shifts is unknown.

58
59 Baseline expectations from global warming suggest that warm-adapted species may
60 increasingly substitute cold-adapted species (De Frenne et al., 2013; Gottfried et al., 2012;
61 Svenning & Sandel, 2013), with some degree of individual species adaptation (Franks et al.,
62 2014; Lavergne et al., 2010). At large scale, biogeographic predictions suggest species
63 displacement via range shifts (Lenoir & Svenning, 2015), with lagged dynamics caused by
64 dispersal and colonization constraints of warm-adapted species to colonize climatic suitable
65 area (Boulangeat et al., 2012; Govaert et al., 2021; Ozinga et al., 2009). Thermophilization is
66 thus the product of different rates of colonization and/or extinction (sensu local extirpation) of
67 warm- vs. cold- adapted species in a community. At one extreme, thermophilization may stem
68 from colonization of warm-adapted species without any extinction of cold-adapted species
69 (Fig.1). Conversely, thermophilization may stem from extinction of cold-adapted species only
70 thus implying biotic erosion of communities rather than community adaptation under climate
71 change (Fig.1).

72
73 Thermophilization effects on local-scale diversity (α -diversity) are straightforward, extinction
74 could cause a loss of species richness and colonization a gain of species richness (Staude et
75 al., 2022; Steinbauer et al., 2018). This change in diversity is particularly documented in
76 mountains forest and summits, where colonization is facilitated (Steinbauer et al., 2018). Less
77 known is how thermophilization causes a decrease of β -diversity, homogenization hereafter.
78 Indeed, thermophilization can be driven by the increase of an already common ubiquitous

79 warm-adapted species, and thus reduces β -diversity (Fig.1.b). Conversely, local extinction-
80 driven thermophilization can homogenize communities if the declining cold-adapted species
81 are rare (Fig.1.b). Understanding which community dynamics drive these processes and how
82 thermophilization is linked with biodiversity changes is thus necessary to understand climate-
83 change induced community shifts (Baeten et al., 2012; Tatsumi et al., 2020, 2021).

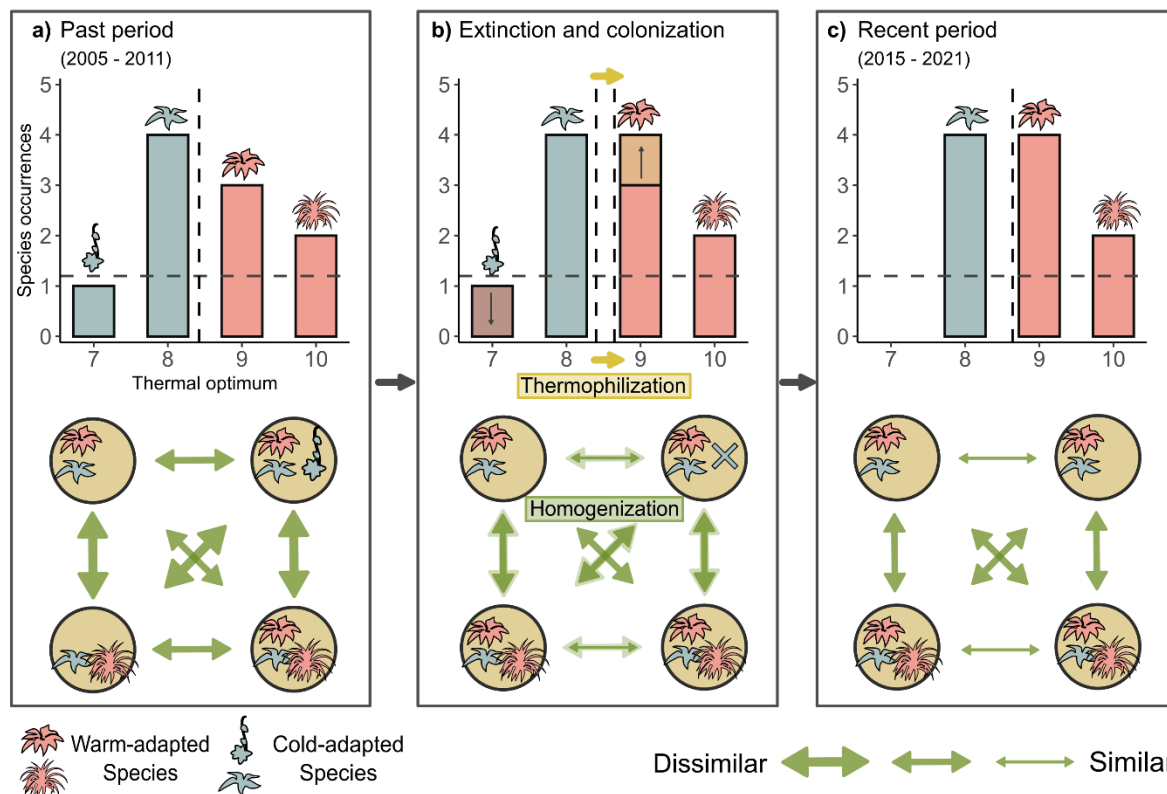
84

85 Here, we unveil the community dynamics (extinction and colonization) responsible for shifts in
86 both thermophilization and β -diversity. We disentangled both β -diversity and thermophilization
87 dynamics based on recent methods to decompose extinction and colonization processes of
88 temporal changes in communities (Tatsumi et al., 2021). We applied our framework to analyze
89 temporal shifts in 12,764 plots (with 745 plant species) of understory forest communities in 80
90 forest ecoregions France (homogenous areas in environmental conditions, a total of 535,218
91 km²), from 2005 to 2021 (IGN, 2013, 2019). We computed the individual contribution of each
92 species to the change in mean thermal optimum (i.e. thermophilization) and in β -diversity (i.e.
93 homogenization) in each ecoregion (Fig1.b). We partitioned those contribution into 4
94 community processes: extinction and colonization of cold and warm-adapted species,
95 respectively.

96

97 With this partitioning we specifically asked: (1) Is there a significant thermophilization of
98 forests, and what community processes drive it? (2) Is there a significant flora homogenization
99 of forests and what community processes drive it? And (3) is mean annual temperature
100 significantly linked to thermophilization and homogenization or their extinction and/or
101 colonization processes? Our initial expectation was that thermophilization is a product of both
102 extinction of cold-adapted species and colonization of warm-adapted species, with faster rates
103 in warmer ecoregions, and that homogenization is pervasive and triggered by abundant warm-
104 adapted species colonization (Merle et al., 2020; Tobias & Monika, 2012; Zwiener et al., 2018).

105



106

107

108

109

110

111

112

113

114

115

116

117

118

119

120

Figure 1: Example of the coupling between thermophilization and homogenization under increasing temperatures (a): An artificial ecoregion comprised of four communities. The ecoregion has two cold and two warm-adapted species depending on whether their thermal optimum is lower or higher than the mean thermal optimum of the ecoregion. The communities are heterogenous as they are all unique. The vertical dotted line represents the mean thermal optimum of the species, the horizontal dotted line represents a threshold differentiating rare from common species (b): An example of thermophilization triggered by the spread of a warm-adapted species and the extinction of one cold-adapted species. The loss of a rare species that made a community unique trigger homogenization, the spread of a common species can also trigger homogenization by increasing similarity with other community (arrow width shrinks). Thermophilization can also heterogenize communities by removing common cold-adapted species or by promoting a rare or absent warm-adapted species (not shown). (c): The resulting ecoregion with a higher mean thermal optimum and more similar communities.

121

2. Results & Discussion

122

Climate-driven extinction of species drives thermophilization

123

124

125

The absolute number of occurrences with low thermal optimum decreased within a decade (2005-2011 vs. 2015-2021, Fig.2). As a consequence, 72 out of the 80 ecoregions had a

126 positive thermophilization rate. The mean thermophilization rate of an ecoregion was 0.012 °C
127 yr⁻¹ (s.d. 0.011, Fig.3.a). This rate was entirely driven by extinction (Fig.3.a) – species which
128 occurrences decreased over time. The thermophilization rate we found is consistent with
129 previous studies of temperate forest understory flora change (Bertrand et al., 2011; Dietz et
130 al., 2020; Govaert et al., 2021; Martin et al., 2019; Richard et al., 2021), that reported rates of
131 c.a 0.010 °C yr⁻¹, a value lagging behind the observed warming rate of c.a 0.025°C yr⁻¹ in our
132 study region (Dietz et al., 2020). These studies, however, did not provide a quantification of
133 the species turnover driving these rates.

134
135 Thermophilization is generally interpreted as the gradual replacement of cold-adapted species
136 by warm-adapted species, which growth and establishment are facilitated by temperature
137 increase (De Frenne et al., 2013). As we measured the extinction contribution to be 0.012 °C
138 yr⁻¹ (s.d. 0.009), we only found evidence of a decrease of occurrences as a driver of the
139 thermophilization. This result was confirmed by a null model in which the change of
140 occurrences of a species is independent of its thermal optimum (Fig.3.a, see methods: null
141 models). Extinction of warm-adapted species was significantly lower compared to this
142 expected random rate. The observed colonization effects on thermophilization were not
143 significantly different from those random rates (Fig.3.a). Our interpretation of an extinction-
144 driven thermophilization was robust to different databases used to infer species thermal
145 optima (Table S1, see methods: null models), and to the uncertainty of thermal optima
146 estimation (Rodríguez-Sánchez et al., 2012) (Table S1, see methods: null models). We also
147 rejected the hypothesis of an overall decrease of occurrences (Fig.2) as an explanation for
148 the significance of the extinction component with a rarefaction model (Table S2, see methods:
149 null models).

150
151 Extinction has already been identified as a key driver of thermophilization in drylands (Pérez-
152 Navarro et al., 2021), via a selection of the most drought-resistant species at the expense of
153 the colder-adapted species after a drought-pulse event. Our results extend this observation to
154 the European Temperate, Mediterranean and Mountainous forests biomes (Extended table.1)
155 over 16 years of continued warming. The Mediterranean and the warmest lowlands ecoregions
156 displayed the fastest thermophilization rates, as we estimated the increase of the extinction
157 component of 0.003 °C yr⁻¹ per rise of degree in MAT (Fig.4.a), up to an extinction component
158 of 0.020 °C yr⁻¹ in the southmost ecoregions (Fig.4.a). This higher extinction rate indicates that
159 thermal stress induced by a warmer climate is sufficient to trigger mortality or impair the
160 establishment of cold-adapted individuals. This finding concurs with projections of species
161 climatic suitability, where extinction is expected at the warm edge of a species distribution
162 (Barbet-Massin et al., 2010; Dullinger et al., 2012; Engler et al., 2011).

163

164 The thermophilization rates we found do not match the climate warming rates during our study
165 period (on average $0.026\text{ }^{\circ}\text{C yr}^{-1}$, Dietz et al., 2020), implying a delay between community
166 dynamics and climate change. This discrepancy could be explained by the lack of colonizing
167 warm-adapted species needed to speed up thermophilization. As our analysis is set at the
168 ecoregion level, our results confirm the lack of migration of understory plants over large areas
169 and triggered by climate change (Fig.4.a). This observation is likely a consequence of the
170 limited dispersal capacities of plants (depending on life cycle, seeds traits etc...) that are not
171 fast enough to follow isotherms shifts induced by climate warming in lowlands ecosystems
172 (Lenoir & Svenning, 2015; Loarie et al., 2009; Serra-Diaz et al., 2014). The only ecoregions
173 where the colonization component drives thermophilization significantly (without exceeding a
174 third of thermophilization) are the mountainous ecoregions (Extended Table 1), concurring
175 with other studies (Bertrand et al., 2011; Lenoir et al., 2008). Indeed, the distance to track
176 shifting isotherms is shorter than in lowlands (Rolland, 2003) which facilitates colonization.
177 Other explanatory factors of the lagged rate could stem from local adaptation of plant
178 populations (Franks et al., 2014; Kubisch et al., 2013; Lavergne et al., 2010) and forest
179 microclimate (De Frenne et al., 2019). Indeed, the temperature buffering of forest canopy
180 slows down thermophilization, as it reduces the exposure of cold-adapted species to stress
181 and extreme events (De Frenne et al., 2019; De Lombaerde et al., 2021; Suggitt et al., 2018;
182 Zellweger et al., 2020). Conversely, warm-adapted species are promoted by canopy opening
183 that increases temperature and light availability (De Frenne et al., 2015; Dietz et al., 2020;
184 Gasperini et al., 2021; Zellweger et al., 2020) However, canopy cover did not influence our
185 results as the mean canopy cover of plots did not meaningfully change between the two
186 periods (mean across ecoregions: past period= 75.9%, present period= 78.5%).

187

188 *Absence of large-scale community homogenization despite extinction of cold-*
189 *adapted species*

190

191 We expected the ecoregion to homogenize toward warmer-adapted communities, concurring
192 with the strong signal of extinction-driven thermophilization (Fig.1). However, homogenization
193 was not a significant trend as only 32 out of the 80 ecoregions displayed a negative $\Delta\beta$ -
194 diversity, whereas 48 showed a positive one. The mean $\Delta\beta$ -diversity across ecoregions was
195 0.33 (s.d. 1.4) and it was not significantly different from 0 (Fig.3.b). The mean β -diversity of an
196 ecoregion in the past period was 12.0 (s.d. 3.5). As a reminder, Whitaker β -diversity (β_w) index
197 reflects the total number of species of the ecoregion when multiplied over the average local
198 (community) richness. The absence of a clear trend in homogenization did not imply a stasis

199 in community dynamics. We found significant contributions of colonization and extinction of
200 warm- and cold-adapted species (Fig.3.b) to changes in β -diversity, except for the extinction
201 of warm-adapted species. These dynamics displayed opposite directions and cancelled each
202 other out, resulting in an overall weak signal of community homogenization.

203

204 Colonization dynamics contributed significantly to heterogenization (mean effect of 1.04 s.d.
205 0.94, Fig.3.b). This implies that the heterogenizing effect of the colonization of rare or new
206 species surpassed the homogenization (β -diversity decrease) caused by the increase of
207 already widespread species. Surprisingly, this effect was explained by the colonization of cold-
208 adapted species (Fig.3.b, 0.84 s.d. 0.68). As no significant increase of cold-adapted species
209 were detected in the thermophilization analysis, this positive contribution is explained by
210 stochastic colonization of rare or previously absent cold-adapted species (Fig.1). The
211 unpredictability of such events may arise from extreme but exceptional values of some species
212 dispersal distance (Vittoz & Engler, 2007), dormant seeds of the seedbank (Gasperini et al.,
213 2021), but also from the limited number of plots in certain ecoregions. With a low number of
214 plots, γ -diversity (total number of species in the ecoregion) is lower, the species partitioning
215 methods will thus be sensitive to local colonization of rare species that affect the γ -diversity.

216

217 Extinction of cold-adapted species, the main driver of community thermophilization (see
218 above), contributed significantly to homogenization (-0.72 s.d. 0.82, Fig.3.b). The magnitude
219 of this contribution is, however, comparable to the colonization effects. This is explained by
220 the decline of rare cold-adapted species strongly contributed to homogenization (-1.95,
221 Extended Fig.2), that was mitigated by simultaneous gains in heterogeneity via the decline of
222 widespread cold-adapted species (1.23, Extended Fig.2). While the widespread cold-adapted
223 species effect on $\Delta\beta$ -diversity was lower, it should not be undermined as it corresponds to
224 species contributing to two third of the thermophilization (Extended Fig.2). Furthermore, the
225 decline of widespread cold-adapted species compensated for the extinction of rare cold-
226 adapted species by reducing local diversity, thus increasing the heterogeneity between plots.
227 This is confirmed by the rarefaction null model we created where the number of total
228 occurrences was kept constant (thus the α -diversity term of the Whitaker β is constant- see
229 methods) displayed a significantly lower $\Delta\beta$ -diversity compared to the original dataset ($\Delta\beta$ -
230 diversity = - 0.32).

231

232 Our results likely reflect transient community dynamics where the beginning of an
233 anthropogenic stressor could initially increase β -diversity by reducing the occurrences of
234 widespread species, but is not acute enough to trigger definitive extinction. This first increase
235 in β -diversity could thus be transitory as every species becomes rarer over time, and

236 eventually become extinct (Socolar et al., 2016). In our case, the contribution of the decline of
237 rare cold-adapted species to homogenization outweighed the positive effect of its colonization
238 counterpart. That is, more rare species declined (with climate change as a driver of this
239 decline) than rare species sporadically colonized. In addition to the thermal stress imposed by
240 climate-change, populations of rare species are isolated from their source population, lack the
241 critical size for maintenance and can be located at the warm edge of its distribution (Leibold &
242 Chase, 2017; Pérez-Navarro et al., 2021).

243

244 The differences in homogenization contribution depending on the relative thermal optimum of
245 a species is indicative of the relationship between thermophilization and β -diversity.
246 Thermophilization is a selective process, in our study, we mostly documented a decline of
247 cold-adapted species with antagonistic effect on β -diversity. The correlation of the
248 homogenization components with MAT (Fig.4.b) is significantly positive and consistent with
249 the correlation of thermophilization with MAT (Fig.4.a). This control of climate over the
250 underlying community dynamics confirms that the thermophilization and homogenization rates
251 could increase with climate change.

252

253

254 *Implications for forest understory in a warming climate*

255

256 Thermophilization is often interpreted as an adaptation of communities to warmer conditions
257 or community substitution (De Frenne et al., 2013; Gottfried et al., 2012), but our results show
258 that thermophilization stems from local extinctions of cold-adapted species, with little
259 substitution from warm adapted species. Indeed, our results show the lack of individual
260 resistance of understory plant species to raising temperature, which exceeds the
261 establishment and dispersal capacities of those plants better adapted to warmer climates. This
262 effect jeopardizes the ecosystems services that the herbaceous layer (Landuyt et al., 2019)
263 and its β -diversity provide (Mori et al., 2018; Tobias & Monika, 2012; Wang et al., 2021). While
264 the effects of an extinction-driven thermophilization on local diversity is clear, how it can cause
265 homogenization is not apparent. We documented a lack of a unidirectional trend of community
266 homogenization, but we observed a rarefaction of cold-adapted species that may trigger
267 homogenization in the future.

268

269 Our consistent finding of extinction being the driving force behind thermophilization calls for
270 increased needs to assess future biodiversity trends as it is positively correlated with MAT. In
271 other ecosystems, where the spread of warm-adapted species can be faster than in lowland

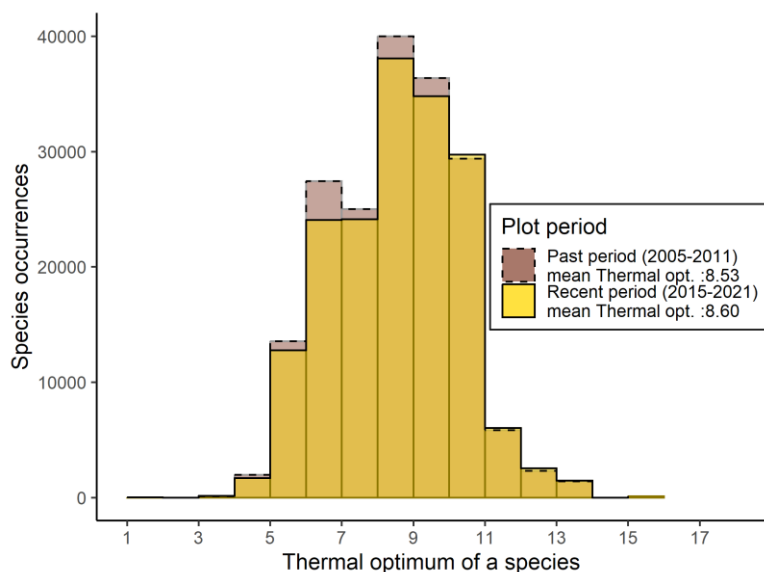
272 forest (e.g. mountains), the effects of β -diversity should still be studied and monitored (Staide
273 et al., 2022; Xu et al., 2023).

274

275 We demonstrated that the extinction of cold-adapted species occurs independently of their
276 rarity. The decline of rare species is pervasive and hard to detect without dedicated
277 conservation studies, but widespread cold-adapted species could be used to bioindicate early
278 sign of climate induced extinctions. The question of whether increased thermophilization and
279 lack of homogenization are transient and respond to the current flora-climate disequilibrium
280 will need further monitoring, but remain critical under future needs to preserve biodiversity.
281 Explicitly unveiling the community dynamics at play to strengthen our capacity to understand
282 and predict community composition under an accelerating warming rate.

283

284



285

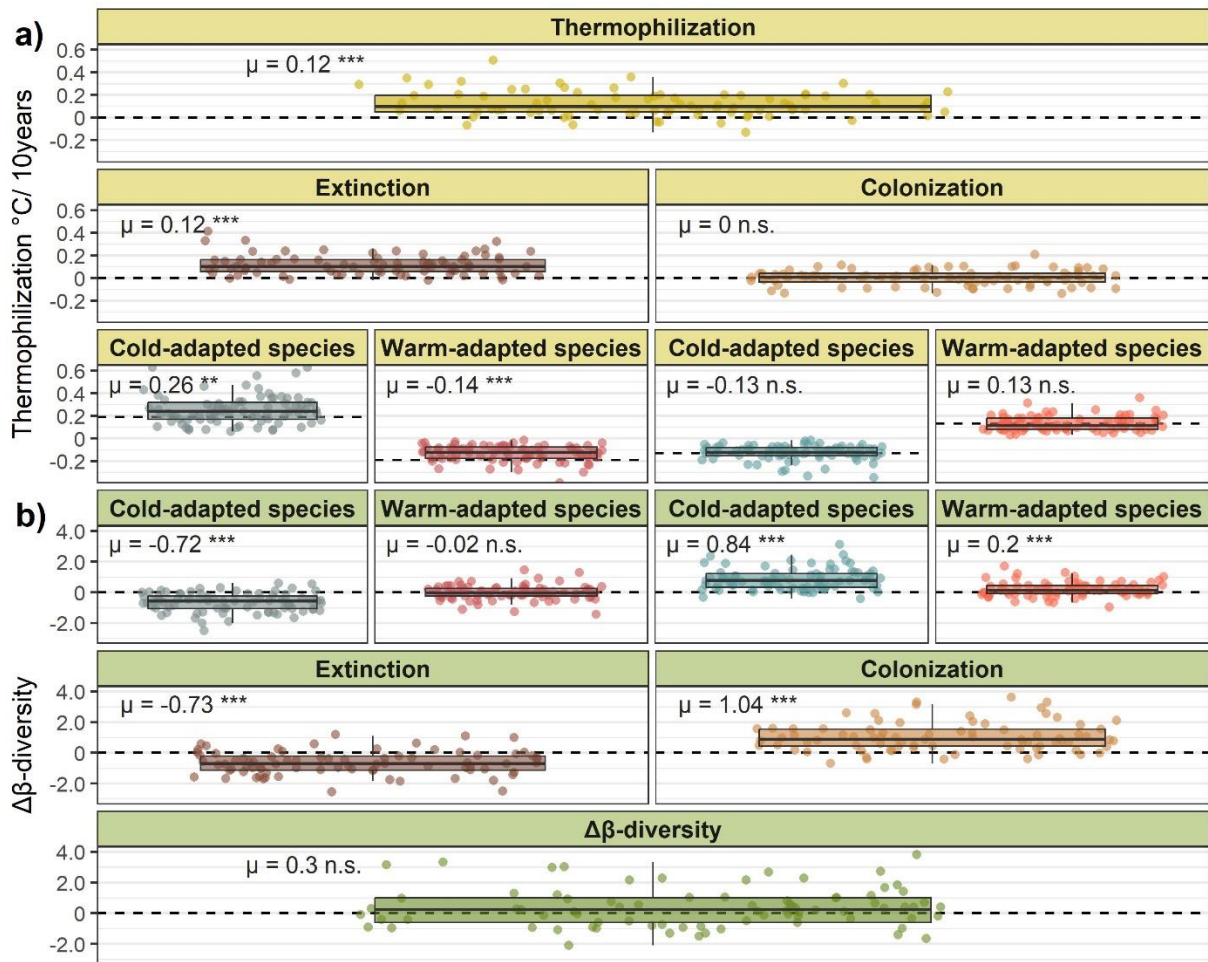
286

287 **Figure 2: Count of species occurrences in the two periods as function of their thermal**
288 **optimum.** The dataset is comprised of 12,764 “past” plots (surveyed in 2005-2011) and
289 12,764 “recent” plots (surveyed in 2015-2021). The thermal optimum of a species is estimated
290 as the mean of the mean annual temperature within a species distribution (Vangansbeke et
291 al., 2021).

292

293

294



295

296

297

298

299

300

301

302

303

304

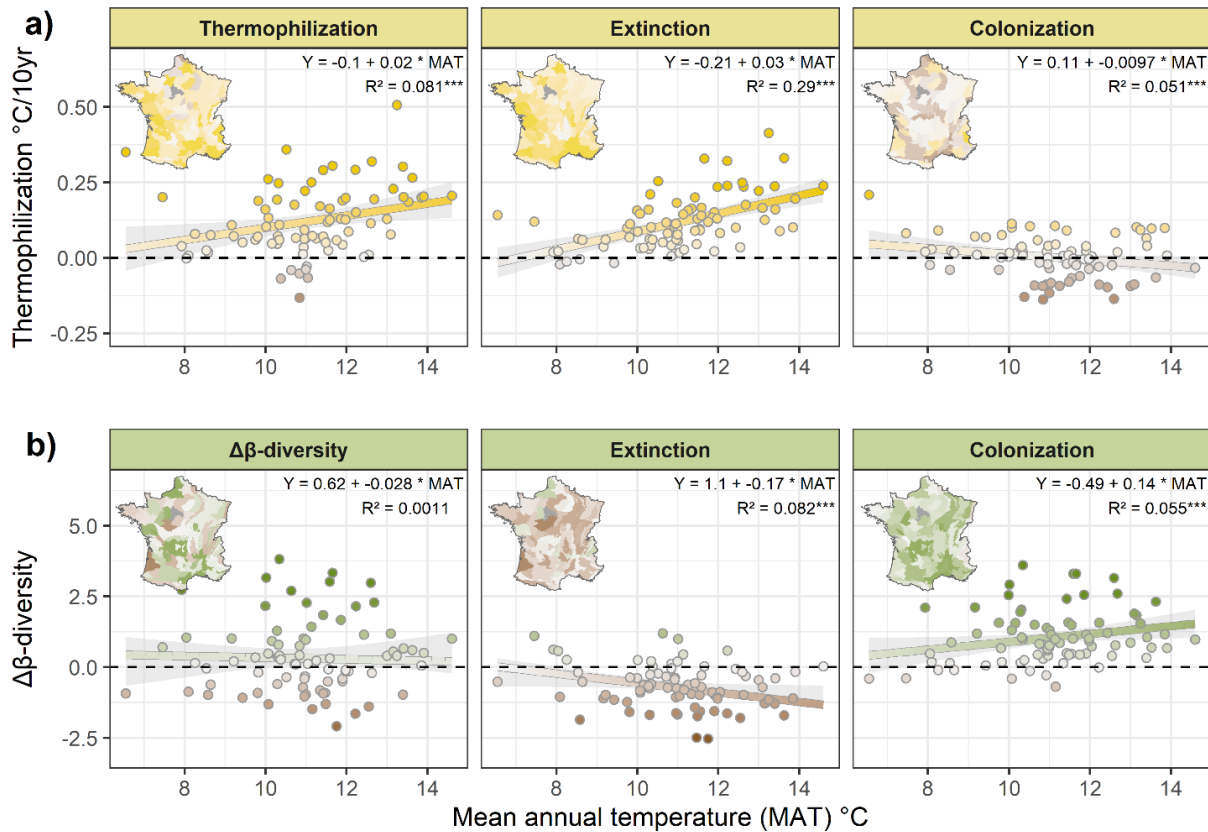
305

306

307

308

Figure 3: Thermophilization (a) and homogenization (b) partition of the 80 studied ecoregions. Change in mean thermal optimum (a) of recorded species and β -diversity (b) (respectively thermophilization and $\Delta\beta$ -diversity) of the 80 ecoregions (represented by a point). Those changes are broken-up in two components: colonization and extinction, estimated from the contribution of species with more or with less occurrences in the recent period. Those components are subsequently divided into the contribution of cold or warm-adapted species, defined as the species with a lower or higher thermal optimum than the mean thermal optimum of the ecoregion in the past period. For each component, the mean value is displayed ($^{\circ}\text{C}$ decades $^{-1}$ for thermophilization, no unit for $\Delta\beta$ -diversity). The statistical difference between this value and a null model (for thermophilization) or 0 (for $\Delta\beta$ -diversity) is also displayed, $p < 0.05$ (*), $p < 0.01$ (**), $p < 0.001$ (***). One outlier ecoregion is not displayed in (b), due to a low number of plots it displayed an extinction component of -4.8 and -5.6 respectively.



309

310 **Figure 4: Relationship of thermophilization (a), β-diversity change (b) and their**
 311 **extinction and colonization components with mean annual temperature (MAT).** One
 312 point represents one ecoregion, the map of the ecoregion with the associated value is
 313 displayed for each component, the color scale of the point and the mapped ecoregion are the
 314 same. One outlier ecoregion is not displayed in (b), due to a low number of plots it displayed
 315 an extinction component of -4.8 and -5.6 respectively. The summary statistics corresponds to
 316 a linear model $Value \sim MAT$, if the MAT coefficient is significant, *** is displayed next to the
 317 R^2 .

318

319

320

321 3. Materials and methods

322 Study region and forest ecoregion

323 Our study area corresponds to metropolitan France (excluding Corsica island), including the
 324 temperate mixed forest biomes, the coniferous mountain biome and the Mediterranean forest
 325 biome. The territory has been divided into 86 forest ecoregions (hereafter ecoregions)
 326 characterized by similar and unique climatic and soil conditions combination (IGN, 2013). We
 327 used those ecoregions to delineate the sampling areas used to study understory flora change

328 and diversity at a wider scale than the plot scale. As they display distinct climate and soil
329 characteristics, we assume the pool of species to be similar within an ecoregion, but differ
330 from the pools of other ecoregions.

331 Lowland ecoregions are characterized by mosaics of forest, meadow and croplands, with a
332 climate ranging from oceanic to semi-continental (contemporary climate range at the
333 ecoregion scale: MAT range=9.4 to 13.9 °C, Precipitation range= 300 to 559 mm yr⁻¹).
334 Mountainous and pre-mountainous ecoregions display higher forest cover and continental
335 mountainous climate, with the exception of the oceanic influence over the Pyrenees (MAT
336 range=6.5 to 12.4 °C, Precipitation range= 409 to 815 mm yr⁻¹). The southmost ecoregions
337 encompass the Mediterranean border from Spain into Italy and display the warmer and dryer
338 climate of European France (MAT range=11.6 to 14.6 °C, Precipitation range= 284 to 451 mm
339 yr⁻¹) (IGN, 2013).

340

341 *Plot selection*

342 We extracted data from the French National Forest Inventory (NFI). We selected the plots
343 from the year 2005 to 2021. The systematic sampling of the NFI is based on 1km-by-1km grid,
344 with one tenth of the grid nodes being surveyed each year. Once the grid is completely
345 surveyed, a new cycle of survey is performed. The plots of the new cycle are thus not a revisit
346 of the previous plots but a new plot performed in a proximity of the node. We extracted from
347 each plots the Mean Annual Temperature from a climate model calibrated with 214 French
348 weather station (MAT) of the 1990-2015 period (Piedallu et al., 2019) and elevation from a
349 25m resolution digital elevation model.

350 We took advantage of the spatial representativeness the systematic sampling offers to study
351 vegetation changes by creating a dataset balanced in sampling intensity and along
352 environmental conditions through time. We assigned plots from the 2005 to 2011 campaign to
353 the “past” category and the plots from the 2015-2021 campaign to the “recent” category. Plots
354 between those two time-frames were removed as their geographically close plot from the new
355 cycle was not available yet. We also removed plots identified as deforested at the time of the
356 survey and plots with less than five species with a known thermal optimum.

357 We then paired “past” and “recent” plots based on several criterion: (1) The distance between
358 the two plots must be less than 2 km, (2) the time interval between plots must be 9 or 10
359 years, (3) the plots must be in the same ecoregion, (4) the difference of elevation of two plots
360 should be less than 50 m. Criteria (1) allowed us to select plots from two NFI cycles of the
361 same node, and compensate for the coordinates fuzziness of the NFI plots (of ± 500m) due to
362 private property protection laws. Furthermore, out of the initial 83 ecoregions, we removed
363 three ecoregions with low number (N<10) of pairs.

364

365 The selection procedure yielded 12,764 pairs of NFI plots separated on average by 9.7 years
366 (Extended Fig.1), distributed in 80 Ecoregions. Ecoregions had a minimum of 15 pairs, a
367 maximum of 1,747. The median value was 104 pairs. In the absence of true remeasurements
368 of past surveys, the selection of geographically close plots to study vegetation changes is the
369 better alternative, but can still misestimate or detect changes where there are none (Chytrý et
370 al., 2014). However, by conducting 80 separate flora change analyses, one per ecoregion,
371 identifying consistent trends across ecoregions, as well as averaging the results limit the risk
372 of misinterpretation.

373

374 *Floristic database*

375 Among dendrometric, canopy cover and soil measurement, the NFI also includes a floristic
376 survey performed in a 15 m radius circle (area = 709 m²). From this survey, we selected
377 vascular plants identified to the species level, and removed trees, as their presence in the
378 understory can be induced by management and they respond slowly to environmental
379 changes (Lenoir et al., 2008). After homogenization of the taxonomy to the TaxRef V13
380 standard (Gargominy, 2022), we assigned to each species a thermal optimum from the
381 ClimPlant V1.2 database (Vangansbeke et al., 2021). Those thermal optima have been
382 computed by averaging the mean annual temperature within the species distribution obtained
383 from European atlases. We also extracted two additional thermal optima (one computed in
384 2005 and one computed in 2019 with updated information and methods) based on Gégout et
385 al. (2005) to test the sensitivity of our results to the source information of thermal optimum
386 estimation.

387 In our 12,764 plot pairs, we recorded 183,608 species occurrences in the past plots, and
388 175,617 species occurrences in the recent plots. We identified 745 different species with a
389 known thermal optimum from ClimPlant V1.2. Those occurrences represented 78% of the total
390 number of occurrences recorded in our plot pairs, showing a large taxonomic coverage of the
391 thermal optimum database.

392

393 *Thermophilization computation and partitioning*

394 To compute thermophilization, we first defined the mean thermal optimum of the recorded
395 species in the “past” and “recent” plots of each ecoregion. To this end, we calculated the
396 weighted mean of the thermal optimum of the species using their occurrence count in the
397 ecoregion, independently of their local abundance. Thermophilization was then obtained by
398 subtracting the “recent” from the “past” occurrence-weighted mean of thermal optimum. As

399 our plots were not exactly separated by 10 years on average, we corrected the
 400 thermophilization rates by the average time difference of the plots to express thermophilization
 401 in degree Celsius per year ($^{\circ}\text{C yr}^{-1}$). This method of computing thermophilization differs from
 402 past studies with permanent plots, where change in mean thermal optimum is computed at
 403 the plot scale through time. Our approach does not investigate plot scale changes (that were
 404 blurred by the semi-permanent nature of our pairs) but allows to study the change of
 405 occurrence rates of species at regional scale under homogenous environmental conditions.
 406 We then computed the individual contribution of a species to thermophilization, contrib_i , with
 407 the following formula:

$$408 \quad \text{Contrib}_i = \frac{(\text{Topt}_i - \text{Topt}_{\text{ecoreg past}}) \cdot (\text{occ}_{i \text{ recent}} - \text{occ}_{i \text{ past}})}{\sum \text{occ}_{\text{recent}}} \quad (1)$$

409 Where Topt_i is the thermal optimum of a species i , $\text{Topt}_{\text{ecoreg past}}$ the weighted mean thermal
 410 optimum of the “past” occurrences, occ_i is the count of plots where the species is recorded in
 411 the “past” and “recent” period, and $\sum \text{occ}_{\text{recent}}$ is the total number of occurrences of the “recent”
 412 period, it allows to scale contrib_i as the two periods will not have an equal number of total
 413 occurrences. Species with equal occurrences in the two periods results in a contrib_i of 0, thus
 414 they do not contribute any further to the computation.

415 When summing every contrib_i , we obtain the thermophilization value of the given ecoregion.
 416 As a result, we can partition the sums of contrib_i into components that can be added to obtain
 417 the thermophilization value. To create the extinction and colonization components, we added
 418 the contrib_i of species with declining occurrences for extinction ($\text{occ}_{i \text{ recent}} - \text{occ}_{i \text{ past}} < 0$), and the
 419 contrib_i of species with increasing occurrences for colonization ($\text{occ}_{i \text{ recent}} - \text{occ}_{i \text{ past}} > 0$). We
 420 subdivided those two components into the contribution of cold and warm-adapted species to
 421 those components. Those subcomponents depend on whether a species is locally cold-
 422 adapted ($\text{Topt}_i - \text{Topt}_{\text{ecoreg past}} < 0$) or warm-adapted ($\text{Topt}_i - \text{Topt}_{\text{ecoreg past}} > 0$) compared to the
 423 weighted mean thermal optimum of the ecoregion $\text{Topt}_{\text{ecoreg past}}$.

424 Consequently, the contribution of the extinction of cold-adapted species will always be positive
 425 (contribute to thermophilization) as denoted by Eq. (1), but the extinction component as a
 426 whole could either be positive or negative (contribute to slow thermophilization), as it also
 427 includes the extinction of warm-adapted species that is negative by design (eq (1)).

428 *Beta-diversity change computation and partitioning*

429 In parallel to the thermophilization analysis, we computed a β -diversity, the Whittaker β_w
 430 metric, for the two periods (Whittaker, 1960). the Whittaker β_w is calculated as described in Eq
 431 (2):

$$432 \quad \beta_w = \frac{\gamma}{\alpha} \quad (2)$$

433 Where γ is the total number of different species recorded in the ecoregion and α is the mean
434 species richness of the plots present in the ecoregion. This metric is more suited to investigate
435 differences between multiple communities than mean of pairwise differences metrics as it
436 accounts for species co-occurrences, and measures heterogeneity by directly assessing the
437 proportionality between local and ecoregion diversity (Baselga, 2010; Socolar et al., 2016;
438 Tatsumi et al., 2021).

439 We computed β -diversity change ($\Delta\beta$ -diversity) at the ecoregion level by subtracting the β_w of
440 the “recent” plots by the β_w of the “past” plots. We then computed the contribution of each
441 species to this change in β -diversity by adapting the methods and code presented in Tatsumi
442 et al. (2021). This method assigns an extinction and colonization component to each species;
443 however, we added those two components to obtain a unique value of contribution to $\Delta\beta$ -
444 diversity per species. As a consequence, a species can decrease β -diversity (homogenize) by
445 declining if it was already rare, or by colonizing if it is an already widespread species.
446 Conversely, the colonization of a rare species, or an extinction of a widespread species have
447 a positive impact on $\Delta\beta$ -diversity (heterogenize). We summed the contribution to $\Delta\beta$ -diversity
448 following the same procedure described in the previous part. This allowed to obtain the
449 contribution to $\Delta\beta$ -diversity of declining species (extinction) and spreading species
450 (colonization), and whether these species were locally cold or warm-adapted, for a total of 4
451 components.

452 As other ecologically relevant processes can lie behind an extinction or a colonization
453 component, e.g. the extinction of a rare species decreases β -diversity whereas the extinction
454 of a common one increases β -diversity, we further split the 4 components into “common” and
455 “rare” species subcomponents. A species is tagged “rare” if its decline reduces β -diversity, its
456 colonization increases it between the two timeframes of our data, and conversely, a species
457 is considered “common” if its decline increases β -diversity and its colonization decreases it
458 (Extended Fig.2).

459 In order to have a comparable set of species and components than the thermophilization
460 analysis, this analysis was done with the subset of species included in the thermal optimum
461 database ClimPlant V1.2.

462

463 We run the thermophilization and the $\Delta\beta$ -diversity analysis and partitioning with the two other
464 thermal optima databases (Gégout et al., 2005) and found similar results and interpretations
465 (Table S3).

466

467 *Null models and bootstrapping*

468 We created two null models to test whether the change of species occurrences is independent
469 of thermal optimum, and to correct the analysis when the two periods did not have an equal
470 number of occurrences.

471

472 To test the independence of species occurrence changes to their respective thermal optimum,
473 we ran 200 iterations of the thermophilization analysis by randomizing the thermal optimum of
474 species drawn from the species pool of each ecoregion. This model (hereafter random thermal
475 optimum model) was used to test its difference with the partitioning result of the original
476 dataset, but the lack of thermophilization in this model demonstrated a link between species
477 occurrences changes and their thermal optima (Table S2).

478

479 The total number of occurrences recorded in our dataset decreased between the two periods
480 despite our sample having a balanced number of “past” and “recent” plots. While this decrease
481 could be caused by true ecological factors such as climate change induced extinction,
482 confounding methodological factors could be also be at play. In our dataset, more plots from
483 the “past” period have been surveyed during the vegetation period (53% in the “past” plots vs
484 49% in the “recent” plot), during this period, species identification is easier and more species
485 will be visible. To account for this potential bias, but also to explore $\Delta\beta$ -diversity in setting
486 without a decrease in mean species richness, we ran both the thermophilization and the β -
487 diversity change analysis by rarefying the occurrences. Specifically, for each ecoregion, we
488 randomly removed occurrences of the period with the most total occurrences to match the
489 total occurrences of the other period. We repeated this resampling and the analysis 200 times,
490 (hereafter the rarefaction null model).

491 With this stricter methodology thermophilization is still estimated at $0.12\text{ }^{\circ}\text{C yr}^{-1}$ (s.d 0.11), the
492 extinction component at $0.11\text{ }^{\circ}\text{C yr}^{-1}$ (s.d 0.07), and the colonization component at $0.01\text{ }^{\circ}\text{C yr}^{-1}$
493 (s.d 0.08) (Table S2).

494 We conducted our main analysis by using the MAT within the distribution of a species as an
495 estimation of its thermal optimum, however the high variability of climate within one distribution
496 induces uncertainties in this estimation (Rodríguez-Sánchez et al., 2012; Vangansbeke et al.,
497 2021). To consider this uncertainty, we ran the analysis 500 times by sampling one climatic
498 grid within the distribution instead provided by Vangansbeke et al., (2021) instead of using the
499 mean. Our results did not change with this method but helped quantify the uncertainties of
500 thermophilization estimation of at the ecoregion scale (Table S2, Rodríguez-Sánchez et al.,
501 2012).

502

503 *Statistical testing*

504 We tested the significance of the seven components (global value, extinction, colonization,
505 and the four subcomponents created with the relative thermal optimum of the species) for the
506 two metrics (thermophilization and $\Delta\beta$ -diversity) with the Wilcoxon signed rank test (Rey &
507 Neuhäuser, 2011). However, we chose a different reference for the test depending on the
508 metrics and what hypothesis we wanted to investigate. We tested the difference between the
509 thermophilization components and the corresponding components of the random thermal
510 optimum model. We tested the difference between the $\Delta\beta$ -diversity with 0 as our null
511 hypothesis was “no change in β -diversity” and unlike thermophilization, the components were
512 not constrained in their value (e.g. the contribution of colonizing warm-adapted species to
513 thermophilization is strictly positive, 0 is not adequate for testing it, but its contribution to $\Delta\beta$ -
514 diversity can be positive or negative).

515 For simplicity, we tested every component of Thermophilization and $\Delta\beta$ -diversity only against
516 0 for the two bootstraps presented in previous section (the random thermal optimum model
517 and the rarefaction null model).

518 We tested the significance and the magnitude of the correlation between thermophilization,
519 $\Delta\beta$ -diversity and their two components (extinction and colonization) with MAT with the use of
520 linear regressions. The applicability of linear regressions was checked via the normality and
521 homoscedasticity of the residuals and the independence to confounding variables following
522 the recommendation of (Zuur et al., 2010).

523 We conducted our analysis in the 4.2.2 R statistical environment (R Core Team, 2019), with
524 ‘data.table’ (Dowle & Srinivasan, 2020), ‘ggplot2’ (Wickham, 2011), ‘sf’ (Pebesma, 2018),
525 ‘ggpubr’ (Kassambara, 2023), ‘foreach’ (Microsoft & Weston, 2022) and the ‘doParallel’
526 (Corporation & Weston, 2022) packages. We were inspired by the ‘ecopart’ method and
527 adapted the code presented by Tatsumi et al., (2021) for the $\Delta\beta$ -diversity partitioning.

528

529 *Data availability*

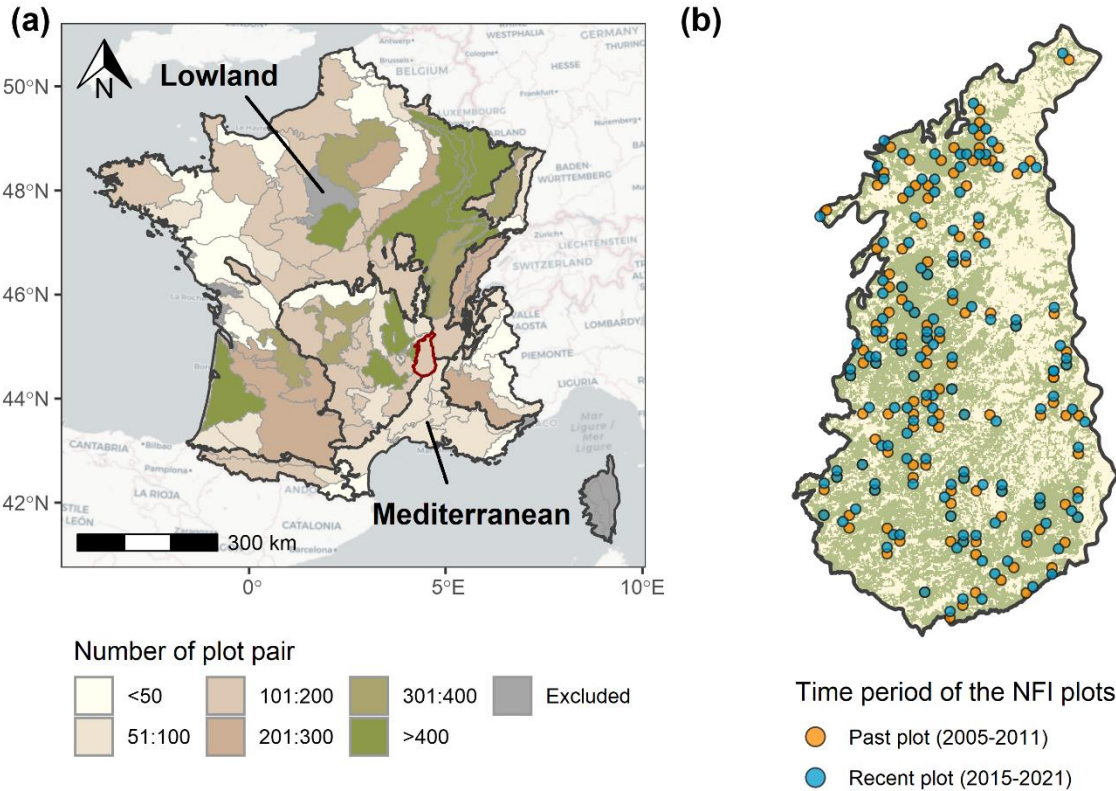
530 French National Forest Inventory data are freely distributed by the French Institute for
531 Geographic and Forest Information (IGN) at <https://inventaire-forestier.ign.fr>

532 The dataset and the code used are available from the authors upon request.

533

534 **4. Extended Data**

535



536

537 **Extended Figure 1:** (a) Map of the 86 forest ecoregions of France, with a colored gradient
 538 representing the number of plot pairs. Three main biomes (Lowland forests, Mediterranean
 539 and Mountain) cluster different ecoregions delineated with bold black lines, the clusters without
 540 a label are mountain ecoregions. The zoomed ecoregion in (b) is outlined in red in (a). (b)
 541 Example of plot pair sampling design- with the blurred localization of the NFI plots, green
 542 represents forested areas.

543

544 **Extended Table 1:** Mean of thermophilization ($^{\circ}\text{C decades}^{-1}$), $\Delta\beta$ -diversity and their
 545 components of one ecoregion depending on their cluster. The number of forest ecoregion
 546 within one cluster and the sum of plot pairs within that cluster is also displayed.

547

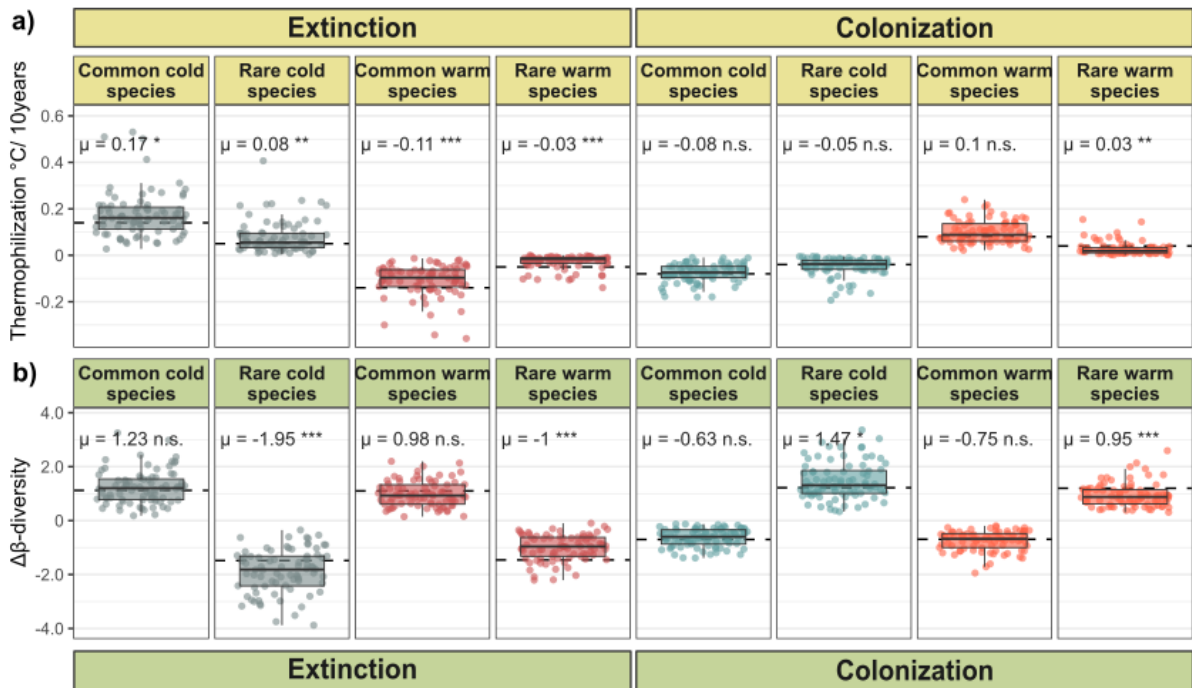
548

Ecoregion cluster	Thermophilization	Extinction	Colonization	$\Delta\beta$ -diversity	Extinction	Colonization	Ecoregion number	Pair number
Lowland	0,01	0,011	-0,001	-0,171	-0,966	0,795	45	8271
Mountain	0,012	0,01	0,002	0,795	-0,412	1,207	29	4116
Mediterranean	0,027	0,029	-0,002	1,498	-0,56	2,058	6	377

549

550

551



552
 553 **Extended Figure 2:** Subsequent partition of the data presented in Fig.3. The contributions to
 554 a) thermophilization ($^{\circ}\text{C decade}^{-1}$), and b) $\Delta\beta$ -diversity (no unit) are partitioned on the basis of
 555 species declining or increasing in occurrences, of their thermal optimum relative to the
 556 ecoregion and whether these species are rare (their decline decrease β -diversity) or common
 557 (their decline increases β -diversity). One point corresponds to one ecoregion. The mean of
 558 each components is displayed. The statistical difference between this value and a null model
 559 (species are assigned a random thermal optimum) is also displayed, $p < 0.05$ (*), $p < 0.01$ (**),
 560 $p < 0.001$ (***).

561
 562

563 5. Acknowledgements

564 The authors are grateful to the French institute for geographic and forest information (IGN) for
 565 providing the NFI data and a precise description of the forest ecoregions. JB was funded by a
 566 joint AgroParisTech and Région Grand- Est grant (grant number 19_GE8_01020p05035) and
 567 JMSD was funded by the ANR-JCJC (Agence Nationale de la Recherche, jeunes chercheuses
 568 et jeunes chercheurs) SEEDFOR (ANR-21-CE32-0003). JMSD acknowledges the support
 569 from NASA for UConn's Ecological Modelling Institute (#80NSSC 22K0883).

570

571 6. References

572
 573 Baeten, L., Vangansbeke, P., Hermy, M., Peterken, G., Vanhuyse, K., & Verheyen, K.
 574 (2012). Distinguishing between turnover and nestedness in the quantification of biotic

575 homogenization. *Biodiversity and Conservation*, 21(6), 1399–1409.
576 <https://doi.org/10.1007/s10531-012-0251-0>

577 Barbet-Massin, M., Thuiller, W., & Jiguet, F. (2010). How much do we overestimate future
578 local extinction rates when restricting the range of occurrence data in climate
579 suitability models? *Ecography*, 33(5), 878–886. <https://doi.org/10.1111/j.1600-0587.2010.06181.x>

581 Baselga, A. (2010). Partitioning the turnover and nestedness components of beta diversity:
582 Partitioning beta diversity. *Global Ecology and Biogeography*, 19(1), 134–143.
583 <https://doi.org/10.1111/j.1466-8238.2009.00490.x>

584 Bertrand, R., Lenoir, J., Piedallu, C., Riofrío-Dillon, G., de Ruffray, P., Vidal, C., Pierrat, J.-
585 C., & Gégout, J.-C. (2011). Changes in plant community composition lag behind
586 climate warming in lowland forests. *Nature*, 479(7374), 517–520.
587 <https://doi.org/10.1038/nature10548>

588 Bertrand, R., Riofrío-Dillon, G., Lenoir, J., Drapier, J., de Ruffray, P., Gégout, J.-C., &
589 Loreau, M. (2016). Ecological constraints increase the climatic debt in forests. *Nature*
590 *Communications*, 7(1), 12643. <https://doi.org/10.1038/ncomms12643>

591 Boulangeat, I., Gravel, D., & Thuiller, W. (2012). Accounting for dispersal and biotic
592 interactions to disentangle the drivers of species distributions and their abundances:
593 The role of dispersal and biotic interactions in explaining species distributions and
594 abundances. *Ecology Letters*, 15(6), 584–593. <https://doi.org/10.1111/j.1461-0248.2012.01772.x>

596 Cholewińska, O., Adamowski, W., & Jaroszewicz, B. (2020). Homogenization of Temperate
597 Mixed Deciduous Forests in Białowieża Forest: Similar Communities Are Becoming
598 More Similar. *Forests*, 11(5), 545. <https://doi.org/10.3390/f11050545>

599 Chytrý, M., Tichý, L., Hennekens, S. M., & Schaminée, J. H. J. (2014). Assessing vegetation
600 change using vegetation-plot databases: A risky business. *Applied Vegetation*
601 *Science*, 17(1), 32–41. <https://doi.org/10.1111/avsc.12050>

602 Comte, L., Muriene, J., & Grenouillet, G. (2014). Species traits and phylogenetic
603 conservatism of climate-induced range shifts in stream fishes. *Nature*
604 *Communications*, 5(1), Article 1. <https://doi.org/10.1038/ncomms6053>

605 Corporation, M., & Weston, S. (2022). *doParallel: Foreach Parallel Adaptor for the “parallel”*
606 *Package*. <https://CRAN.R-project.org/package=doParallel>

607 De Frenne, P., Rodríguez-Sánchez, F., Coomes, D. A., Baeten, L., Verstraeten, G., Vellend,
608 M., Bernhardt-Romermann, M., Brown, C. D., Brunet, J., Cornelis, J., Decocq, G. M.,
609 Dierschke, H., Eriksson, O., Gilliam, F. S., Hedl, R., Heinken, T., Hermy, M.,
610 Hommel, P., Jenkins, M. A., ... Verheyen, K. (2013). Microclimate moderates plant
611 responses to macroclimate warming. *Proceedings of the National Academy of*
612 *Sciences*, 110(46), 18561–18565. <https://doi.org/10.1073/pnas.1311190110>

613 De Frenne, P., Rodríguez-Sánchez, F., De Schrijver, A., Coomes, D. A., Hermy, M.,
614 Vangansbeke, P., & Verheyen, K. (2015). Light accelerates plant responses to
615 warming. *Nature Plants*, 1(9), 1–3. <https://doi.org/10.1038/nplants.2015.110>

616 De Frenne, P., Zellweger, F., Rodríguez-Sánchez, F., Scheffers, B. R., Hylander, K., Luoto,
617 M., Vellend, M., Verheyen, K., & Lenoir, J. (2019). Global buffering of temperatures
618 under forest canopies. *Nature Ecology & Evolution*, 3(5), 744–749.
619 <https://doi.org/10.1038/s41559-019-0842-1>

620 De Lombaerde, E., Vangansbeke, P., Lenoir, J., Van Meerbeek, K., Lembrechts, J.,
621 Rodríguez-Sánchez, F., Luoto, M., Scheffers, B., Haesen, S., Aalto, J., Christiansen,
622 D. M., De Pauw, K., Depauw, L., Govaert, S., Greiser, C., Hampe, A., Hylander, K.,

623 Klinges, D., Koelemeijer, I., ... De Frenne, P. (2021). Maintaining forest cover to
624 enhance temperature buffering under future climate change. *Science of The Total*
625 *Environment*, 151338. <https://doi.org/10.1016/j.scitotenv.2021.151338>

626 Dietz, L., Collet, C., Dupouey, J.-L., Lacombe, E., Laurent, L., & Gégout, J.-C. (2020).
627 Windstorm-induced canopy openings accelerate temperate forest adaptation to
628 global warming. *Global Ecology and Biogeography*.
629 <https://doi.org/10.1111/geb.13177>

630 Dowle, M., & Srinivasan, A. (2020). *data.table: Extension of `data.frame`*. [https://CRAN.R-](https://CRAN.R-project.org/package=data.table)
631 [project.org/package=data.table](https://CRAN.R-project.org/package=data.table)

632 Dullinger, S., Gattringer, A., Thuiller, W., Moser, D., Zimmermann, N. E., Guisan, A., Willner,
633 W., Plutzer, C., Leitner, M., Mang, T., Caccianiga, M., Dirnböck, T., Ertl, S., Fischer,
634 A., Lenoir, J., Svenning, J.-C., Psomas, A., Schmatz, D. R., Silc, U., ... Hülber, K.
635 (2012). Extinction debt of high-mountain plants under twenty-first-century climate
636 change. *Nature Climate Change*, 2(8), Article 8. <https://doi.org/10.1038/nclimate1514>

637 Engler, R., Randin, C. F., Thuiller, W., Dullinger, S., Zimmermann, N. E., Araújo, M. B.,
638 Pearman, P. B., Le Lay, G., Piedallu, C., Albert, C. H., Choler, P., Coldea, G., De
639 LAMO, X., Dirnböck, T., Gégout, J.-C., Gómez-García, D., Grytnes, J.-A., Heegaard,
640 E., Høistad, F., ... Guisan, A. (2011). 21st century climate change threatens
641 mountain flora unequally across Europe: CLIMATE CHANGE IMPACTS ON
642 MOUNTAIN FLORAE. *Global Change Biology*, 17(7), 2330–2341.
643 <https://doi.org/10.1111/j.1365-2486.2010.02393.x>

644 Franks, S. J., Weber, J. J., & Aitken, S. N. (2014). Evolutionary and plastic responses to
645 climate change in terrestrial plant populations. *Evolutionary Applications*, 7(1), 123–
646 139. <https://doi.org/10.1111/eva.12112>

647 Gargominy, O. (2022). *TAXREF v13.0, référentiel taxonomique pour la France*. [Data set].
648 UMS PatriNat (OFB-CNRS-MNHN), Paris. <https://doi.org/10.15468/VQUEAM>

649 Gasperini, C., Carrari, E., Govaert, S., Meeussen, C., De Pauw, K., Plue, J., Sanczuk, P.,
650 Vanneste, T., Vangansbeke, P., Jacopetti, G., De Frenne, P., & Selvi, F. (2021).
651 Edge effects on the realised soil seed bank along microclimatic gradients in
652 temperate European forests. *Science of The Total Environment*, 798, 149373.
653 <https://doi.org/10.1016/j.scitotenv.2021.149373>

654 Gégout, J.-C., Coudun, C., Bailly, G., & Jabiol, B. (2005). EcoPlant: A forest site database
655 linking floristic data with soil and climate variables. *Journal of Vegetation Science*,
656 16(2), 257–260. <https://doi.org/10.1111/j.1654-1103.2005.tb02363.x>

657 Gottfried, M., Pauli, H., Futschik, A., Akhalkatsi, M., Barančok, P., Benito Alonso, J. L.,
658 Coldea, G., Dick, J., Erschbamer, B., Fernández Calzado, M. R., Kazakis, G., Krajčič,
659 J., Larsson, P., Mallaun, M., Michelsen, O., Moiseev, D., Moiseev, P., Molau, U.,
660 Merzouki, A., ... Grabherr, G. (2012). Continent-wide response of mountain
661 vegetation to climate change. *Nature Climate Change*, 2(2), Article 2.
662 <https://doi.org/10.1038/nclimate1329>

663 Govaert, S., Vangansbeke, P., Blondeel, H., Steppe, K., Verheyen, K., & De Frenne, P.
664 (2021). Rapid thermophilization of understorey plant communities in a 9 year-long
665 temperate forest experiment. *Journal of Ecology*. [https://doi.org/10.1111/1365-](https://doi.org/10.1111/1365-2745.13653)
666 [2745.13653](https://doi.org/10.1111/1365-2745.13653)

667 IGN. (2013). *Fiches descriptives des grandes régions écologiques (GRECO) et des*
668 *sylvoécorégions (SER)*. <https://inventaire-forestier.ign.fr/spip.php?article773>

669 IGN. (2019, December 1). Le mémento de l'inventaire forestier. *Institut National de*
670 *l'Information Géographique et Forestière*.
671 <http://www.ign.fr/institut/publications/memento-linventaire-forestier>
672 Kassambara, A. (2023). *ggpubr: "ggplot2" Based Publication Ready Plots*. [https://CRAN.R-](https://CRAN.R-project.org/package=ggpubr)
673 [project.org/package=ggpubr](https://CRAN.R-project.org/package=ggpubr)
674 Kubisch, A., Degen, T., Hovestadt, T., & Poethke, H. J. (2013). Predicting range shifts under
675 global change: The balance between local adaptation and dispersal. *Ecography*,
676 36(8), 873–882. <https://doi.org/10.1111/j.1600-0587.2012.00062.x>
677 Kuhn, E., & Gégout, J. (2019). Highlighting declines of cold-demanding plant species in
678 lowlands under climate warming. *Ecography*, 42(1), 36–44.
679 <https://doi.org/10.1111/ecog.03469>
680 Landuyt, D., De Lombaerde, E., Perring, M. P., Hertzog, L. R., Ampoorter, E., Maes, S. L.,
681 De Frenne, P., Ma, S., Proesmans, W., Blondeel, H., Sercu, B. K., Wang, B., Wasof,
682 S., & Verheyen, K. (2019). The functional role of temperate forest understorey
683 vegetation in a changing world. *Global Change Biology*, 25(11), 3625–3641.
684 <https://doi.org/10.1111/gcb.14756>
685 Lavergne, S., Mouquet, N., Thuiller, W., & Ronce, O. (2010). Biodiversity and Climate
686 Change: Integrating Evolutionary and Ecological Responses of Species and
687 Communities. *Annual Review of Ecology, Evolution, and Systematics*, 41(1), 321–
688 350. <https://doi.org/10.1146/annurev-ecolsys-102209-144628>
689 Leibold, M. A., & Chase, J. M. (2017). *Metacommunity Ecology, Volume 59*. Princeton
690 University Press.
691 Lenoir, J., Gégout, J. C., Marquet, P. A., Ruffray, P. de, & Brisse, H. (2008). A Significant
692 Upward Shift in Plant Species Optimum Elevation During the 20th Century. *Science*,
693 320(5884), 1768–1771. <https://doi.org/10.1126/science.1156831>
694 Lenoir, J., & Svenning, J.-C. (2015). Climate-related range shifts – a global multidimensional
695 synthesis and new research directions. *Ecography*, 38(1), 15–28.
696 <https://doi.org/10.1111/ecog.00967>
697 Loarie, S. R., Duffy, P. B., Hamilton, H., Asner, G. P., Field, C. B., & Ackerly, D. D. (2009).
698 The velocity of climate change. *Nature*, 462(7276), 1052–1055.
699 <https://doi.org/10.1038/nature08649>
700 Martin, G., Devictor, V., Motard, E., Machon, N., & Porcher, E. (2019). Short-term climate-
701 induced change in French plant communities. *Biology Letters*, 15(7), 20190280.
702 <https://doi.org/10.1098/rsbl.2019.0280>
703 Merle, H., Garmendia, A., Hernández, H., & Ferriol, M. (2020). Vegetation change over a
704 period of 46 years in a Mediterranean mountain massif (Penyagolosa, Spain).
705 *Applied Vegetation Science*, 23(4), 495–507. <https://doi.org/10.1111/avsc.12507>
706 Microsoft, & Weston, S. (2022). *foreach: Provides Foreach Looping Construct*.
707 <https://CRAN.R-project.org/package=foreach>
708 Mori, A. S., Isbell, F., & Seidl, R. (2018). β -Diversity, Community Assembly, and Ecosystem
709 Functioning. *Trends in Ecology & Evolution*, 33(7), 549–564.
710 <https://doi.org/10.1016/j.tree.2018.04.012>
711 Olden, J. D., & Rooney, T. P. (2006). On defining and quantifying biotic homogenization.
712 *Global Ecology and Biogeography*, 15(2), 113–120. [https://doi.org/10.1111/j.1466-](https://doi.org/10.1111/j.1466-822X.2006.00214.x)
713 [822X.2006.00214.x](https://doi.org/10.1111/j.1466-822X.2006.00214.x)
714 Ozinga, W. A., Römermann, C., Bekker, R. M., Prinzing, A., Tamis, W. L. M., Schaminée, J.
715 H. J., Hennekens, S. M., Thompson, K., Poschlod, P., Kleyer, M., Bakker, J. P., &
716 van Groenendael, J. M. (2009). Dispersal failure contributes to plant losses in NW

717 Europe. *Ecology Letters*, 12(1), 66–74. <https://doi.org/10.1111/j.1461->
718 0248.2008.01261.x

719 Pebesma, E. (2018). Simple Features for R: Standardized Support for Spatial Vector Data.
720 *The R Journal*, 10(1), 439–446. <https://doi.org/10.32614/RJ-2018-009>

721 Pérez-Navarro, M. Á., Serra-Diaz, J. M., Svenning, J., Esteve-Selma, M. Á., Hernández-
722 Bastida, J., & Lloret, F. (2021). Extreme drought reduces climatic disequilibrium in
723 dryland plant communities. *Oikos*. <https://doi.org/10.1111/oik.07882>

724 Piedallu, C., Chéret, V., Denux, J. P., Perez, V., Azcona, J. S., Seynave, I., & Gégout, J. C.
725 (2019). Soil and climate differently impact NDVI patterns according to the season and
726 the stand type. *Science of The Total Environment*, 651, 2874–2885.
727 <https://doi.org/10.1016/j.scitotenv.2018.10.052>

728 R Core Team. (2019). *R: A Language and Environment for Statistical Computing*. R
729 Foundation for Statistical Computing. <https://www.R-project.org/>

730 Reu, J. C., Catano, C. P., Spasojevic, M. J., & Myers, J. A. (2022). Beta diversity as a driver
731 of forest biomass across spatial scales. *Ecology*, 103(10).
732 <https://doi.org/10.1002/ecy.3774>

733 Rey, D., & Neuhäuser, M. (2011). Wilcoxon-Signed-Rank Test. In M. Lovric (Ed.),
734 *International Encyclopedia of Statistical Science* (pp. 1658–1659). Springer.
735 https://doi.org/10.1007/978-3-642-04898-2_616

736 Richard, B., Dupouey, J.-L., Corcket, E., Alard, D., Archaux, F., Aubert, M., Boulanger, V.,
737 Gillet, F., Langlois, E., Macé, S., Montpied, P., Beauvils, T., Begeot, C., Behr, P.,
738 Boissier, J.-M., Camaret, S., Chevalier, R., Decocq, G., Dumas, Y., ... Lenoir, J.
739 (2021). The climatic debt is growing in the understorey of temperate forests: Stand
740 characteristics matter. *Global Ecology and Biogeography*, n/a(n/a).
741 <https://doi.org/10.1111/geb.13312>

742 Rodríguez-Sánchez, F., De Frenne, P., & Hampe, A. (2012). Uncertainty in thermal
743 tolerances and climatic debt. *Nature Climate Change*, 2(9), 636–637.
744 <https://doi.org/10.1038/nclimate1667>

745 Rolland, C. (2003). Spatial and Seasonal Variations of Air Temperature Lapse Rates in
746 Alpine Regions. *Journal of Climate*, 16(7), 1032–1046. <https://doi.org/10.1175/1520->
747 0442(2003)016<1032:SASVOA>2.0.CO;2

748 Sala, O. E., Chapin, F. S., Armesto, J. J., Berlow, E., Bloomfield, J., Dirzo, R., Huber-
749 Sanwald, E., Huenneke, L. F., Jackson, R. B., Kinzig, A., Leemans, R., Lodge, D. M.,
750 Mooney, H. A., Oesterheld, M., Poff, N. L., Sykes, M. T., Walker, B. H., Walker, M., &
751 Wall, D. H. (2000). Global biodiversity scenarios for the year 2100. *Science (New*
752 *York, N. Y.)*, 287(5459), 1770–1774. <https://doi.org/10.1126/science.287.5459.1770>

753 Serra-Diaz, J. M., Franklin, J., Ninyerola, M., Davis, F. W., Syphard, A. D., Regan, H. M., &
754 Ikegami, M. (2014). Bioclimatic velocity: The pace of species exposure to climate
755 change. *Diversity and Distributions*, 20(2), 169–180.
756 <https://doi.org/10.1111/ddi.12131>

757 Socolar, J. B., Gilroy, J. J., Kunin, W. E., & Edwards, D. P. (2016). How Should Beta-
758 Diversity Inform Biodiversity Conservation? *Trends in Ecology & Evolution*, 31(1),
759 67–80. <https://doi.org/10.1016/j.tree.2015.11.005>

760 Staude, I. R., Pereira, H. M., Daskalova, G. N., Bernhardt-Römermann, M., Diekmann, M.,
761 Pauli, H., Van Calster, H., Vellend, M., Bjorkman, A. D., Brunet, J., De Frenne, P.,
762 Hédli, R., Jandt, U., Lenoir, J., Myers-Smith, I. H., Verheyen, K., Wipf, S., Wulf, M.,
763 Andrews, C., ... Baeten, L. (2022). Directional turnover towards larger-ranged plants

764 over time and across habitats. *Ecology Letters*, 25(2), 466–482.
765 <https://doi.org/10.1111/ele.13937>

766 Steinbauer, M. J., Grytnes, J.-A., Jurasinski, G., Kulonen, A., Lenoir, J., Pauli, H., Rixen, C.,
767 Winkler, M., Bardy-Durchhalter, M., Barni, E., Bjorkman, A. D., Breiner, F. T., Burg,
768 S., Czortek, P., Dawes, M. A., Delimat, A., Dullinger, S., Erschbamer, B., Felde, V.
769 A., ... Wipf, S. (2018). Accelerated increase in plant species richness on mountain
770 summits is linked to warming. *Nature*, 556(7700), Article 7700.
771 <https://doi.org/10.1038/s41586-018-0005-6>

772 Suggitt, A. J., Wilson, R. J., Isaac, N. J. B., Beale, C. M., Auffret, A. G., August, T., Bennie,
773 J. J., Crick, H. Q. P., Duffield, S., Fox, R., Hopkins, J. J., Macgregor, N. A., Morecroft,
774 M. D., Walker, K. J., & Maclean, I. M. D. (2018). Extinction risk from climate change
775 is reduced by microclimatic buffering. *Nature Climate Change*, 8(8), Article 8.
776 <https://doi.org/10.1038/s41558-018-0231-9>

777 Svenning, J.-C., & Sandel, B. (2013). Disequilibrium vegetation dynamics under future
778 climate change. *American Journal of Botany*, 100(7), 1266–1286.
779 <https://doi.org/10.3732/ajb.1200469>

780 Tatsumi, S., Iritani, R., & Cadotte, M. W. (2021). Temporal changes in spatial variation:
781 Partitioning the extinction and colonisation components of beta diversity. *Ecology*
782 *Letters*. <https://doi.org/10.1111/ele.13720>

783 Tatsumi, S., Strengbom, J., Čugunovs, M., & Kouki, J. (2020). Partitioning the colonization
784 and extinction components of beta diversity across disturbance gradients. *Ecology*,
785 101(12), e03183. <https://doi.org/10.1002/ecy.3183>

786 Tobias, N., & Monika, W. (2012). Does taxonomic homogenization imply functional
787 homogenization in temperate forest herb layer communities? *Plant Ecology*, 213(3),
788 431–443. <https://doi.org/10.1007/s11258-011-9990-3>

789 Vangansbeke, P., Máliš, F., Hédli, R., Chudomelová, M., Vild, O., Wulf, M., Jahn, U., Welk,
790 E., Rodríguez-Sánchez, F., & Frenne, P. D. (2021). ClimPlant: Realized climatic
791 niches of vascular plants in European forest understoreys. *Global Ecology and*
792 *Biogeography*, 30(6), 1183–1190. <https://doi.org/10.1111/geb.13303>

793 Vittoz, P., & Engler, R. (2007). Seed dispersal distances: A typology based on dispersal
794 modes and plant traits. *Botanica Helvetica*, 117(2), 109–124.
795 <https://doi.org/10.1007/s00035-007-0797-8>

796 Wang, S., Loreau, M., Mazancourt, C., Isbell, F., Beierkuhnlein, C., Connolly, J.,
797 Deutschman, D. H., Doležal, J., Eisenhauer, N., Hector, A., Jentsch, A., Kreyling, J.,
798 Lanta, V., Lepš, J., Polley, H. W., Reich, P. B., Ruijven, J., Schmid, B., Tilman, D., ...
799 Craven, D. (2021). Biotic homogenization destabilizes ecosystem functioning by
800 decreasing spatial asynchrony. *Ecology*, 102(6). <https://doi.org/10.1002/ecy.3332>

801 Whittaker, R. H. (1960). Vegetation of the Siskiyou Mountains, Oregon and California.
802 *Ecological Monographs*, 30(3), 279–338. <https://doi.org/10.2307/1943563>

803 Wickham, H. (2011). Ggplot2. *WIREs Computational Statistics*, 3(2), 180–185.
804 <https://doi.org/10.1002/wics.147>

805 Xu, W.-B., Blowes, S. A., Brambilla, V., Chow, C. F. Y., Fontrodona-Eslava, A., Martins, I. S.,
806 McGlenn, D., Moyes, F., Sagouis, A., Shimadzu, H., van Klink, R., Magurran, A. E.,
807 Gotelli, N. J., McGill, B. J., Dornelas, M., & Chase, J. M. (2023). Regional occupancy
808 increases for widespread species but decreases for narrowly distributed species in
809 metacommunity time series. *Nature Communications*, 14(1), Article 1.
810 <https://doi.org/10.1038/s41467-023-37127-2>

811 Zellweger, F., De Frenne, P., Lenoir, J., Vangansbeke, P., Verheyen, K., Bernhardt-
812 Römermann, M., Baeten, L., Hédli, R., Berki, I., Brunet, J., Van Calster, H.,
813 Chudomelová, M., Decocq, G., Dirnböck, T., Durak, T., Heinken, T., Jaroszewicz, B.,
814 Kopecký, M., Máliš, F., ... Coomes, D. (2020). Forest microclimate dynamics drive
815 plant responses to warming. *Science*, 368(6492), 772–775.
816 <https://doi.org/10.1126/science.aba6880>
817 Zuur, A. F., Ieno, E. N., & Elphick, C. S. (2010). A protocol for data exploration to avoid
818 common statistical problems. *Methods in Ecology and Evolution*, 1(1), 3–14.
819 <https://doi.org/10.1111/j.2041-210X.2009.00001.x>
820 Zwiener, V. P., Lira-Noriega, A., Grady, C. J., Padiá, A. A., & Vitule, J. R. S. (2018). Climate
821 change as a driver of biotic homogenization of woody plants in the Atlantic Forest.
822 *Global Ecology and Biogeography*, 27(3), 298–309.
823 <https://doi.org/10.1111/geb.12695>
824
825